Special Issue on Proceedings of International Virtual Conference, Recent Materials for, Engineering Applications and Sustainable Environment, December 2020. International Journal of Aquatic Science, Volume 11, Issue 1, 2020.

Design and thermal analysis of partial ceramic coated piston of spark ignition (SI) Engine

[1]S.Selva Kumar, [2]P. Karthi, [3]S.Bairavi, R. Rosy Subha Hannah[4]
[1,2,3&4]Assistant Professor, Department of Aeronautical Engineering
Nehru Institute of Technology, Coimbatore.
nitselvakumar@nehrucolleges.com[1]

Abstract:-This paper is to determine the temperature and the stress distributions in a partial ceramic coated spark ignition (SI) engine piston and reduce the mass of the piston for improving engine operating parameters. Our aim of this paper is to determine the temperature and the stress distributions in a partial ceramic coated spark ignition (SI) engine piston. Effects of coating thickness and width on temperature and stress distributions were investigated including comparisons with results from an uncoated piston. Thermal analysis is investigated on a conventional (uncoated) SI engine piston, made of Al-Si alloy and steel. Secondly, thermal analysis is performed on piston, coated with MgO-ZrO2 material by means of using a commercial code, namely ANSYS. Finally, the results of different pistons will be compared. The effects of coatings on the thermal behavior of the piston are to be investigated and improved.

Introduction

The thermal barrier coating andconstructional change to the aluminum piston crown results in a reduction in the substrate temperature, it may be possible to return the aluminum piston to historic durability levels at the higher engine output levels. The analysis needed a clear definition of the material properties, selection of element, boundary conditions and initial conditions. For which the certain data are calculated using the petrol engine cycle and some are taken from the literatures. All the data assumed in the analysis are theoretical values and hence the analysis is purely theoretical. With the analysis done the results are used to fix a benchmark for carrying out the experimental analysis with the coating of a thermal barrier (PSZ in this case).

Table 1: properties of cast aluminium alloy

Material property	Al Alloy
Thermal conductivity, k (W/mK)	155
Density, ρ (kg/m3)	2700
Specific heat, C (J/kg K)	965
Coefficient of thermal expansion (1/k)	19.5×103
Young's modulus, E (Mpa)	90×103
Yield strength (Mpa)	410
Poisson's ratio	0.3

The piston is made of cast aluminium alloy (AlSi). Its material property is presented in table 1 It has good strength and hardness at elevated temperatures with good wear resistance.

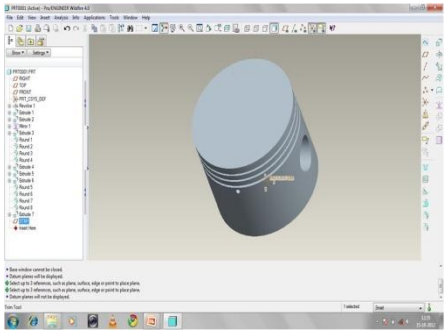

Figure:1 Existing Piston

2. Component modeling

The piston is modeled in PRO-E WILDFIRE-4.0, which is one of the most effective modeling packages. IGES (Initial

Special Issue on Proceedings of International Virtual Conference, Recent Materials for, Engineering Applications and Sustainable Environment, December 2020. International Journal of Aquatic Science, Volume 11, Issue 1, 2020.

Graphics Exchange Specification) is the ANSI standard that defines a natural format for the exchange of information between CAD/CAM systems with an IGES translator. The both existing and modified piston was modeled in PRO-E wildfire 4.0 as per dimensions respectively.

Finite element meshing and analysis

Using SOLID 70 brick element it is meshed as shown in fig.3. As temperature gradients are higher in the combustion chamber therefore a relatively fine mesh is used at the combustion chamber as illustrated in Fig. Away from the combustion chamber centre, the element size gradually increases.

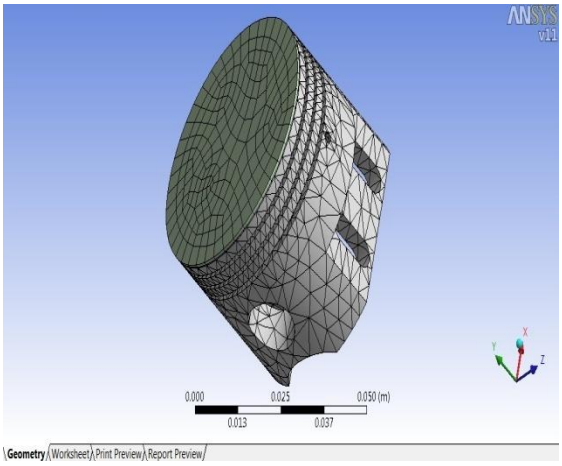

Figure: 2 Meshed View

Post processing

Once the boundary conditions are applied, the problem is solved using the Ansys 11.0 solver. The results obtained are temperature distribution, heat flux, deflection and total stress.

Solution phase

In this phase, initial conditions, boundary conditions and thermal loads are applied as explained below and finally solved to obtain results.Initial and boundary conditions includes thermal and structural conditions. Since the problem is a steady state analysis, the initial condition is the temperature of the piston body only. The initial temperature of the piston is assumed to be 60^{o}C (333K). This assumption is taken with the base that the lubricating oil has the least temperature and acts as the main sink in the system and hence the initial piston temperature at steady state is assume to be equal to the lubrication oil temperature.

Thermal analysis and thermal boundary condition

There are four boundary conditions applied to the model i.e. four convectional heat transfers occurring during the analysis. They are shown in the fig. 4 to fig. 8 below. he first region is the piston head indicated in red. This is where the combustion occurs. Here convectional heat transfer occurs from the working medium to the piston. The working medium above the piston contains a mixture of compressed air, un-burnt fuel and burnt gases at eh moment when the combustion begins. But during that time it is assumed that there would be layers created as shown below. Hence an assumption is made that there would be a one millimeter thin layer of compressed air present over the piston surface. With this a model of a thin air cap having same contour of the piston head is made to find the effective temperature of the gas touching the piston for convection. The model is analysed in Ansys with the boundary conditions as shown in the Figure:. 4 The temperature required to determine the boundary conditions is calculated based on the theoretical Otto cycle and the heat transfer coefficient acting on the top of the piston is calculated by the governing equation.

Table 2: Temperature Distribution

Material	Coating Thickness (mm)	Total Thickness of Coating (mm)	Temperature (^oC)	
			MAX	MIN
NiCrAl (Bond coat)	3	10	504.04	59.342
MgZrO3 (Ceramic)	7			

$$h_{gas} = C_1 V_c^{-0.06} P^{0.8} T^{-0.4} (V_p + C_2)^{0.8}$$

At the end of compression

$$h_{gas} = 2206.257 \frac{W}{m^2 K}$$

At the power stroke

$$h_{gas} = 1736.9985 \frac{W}{m^2 K}$$

Where, C_1 – Constant = 130

C_2 – Constant = 1.4

V_c – Instantaneous cylinder volume (m^3)

V_p – Mean Piston Speed (m/sec)

T – Instantaneous Mean Gas Temperature (K)

P – Instantaneous Cylinder Pressure (Mpa)

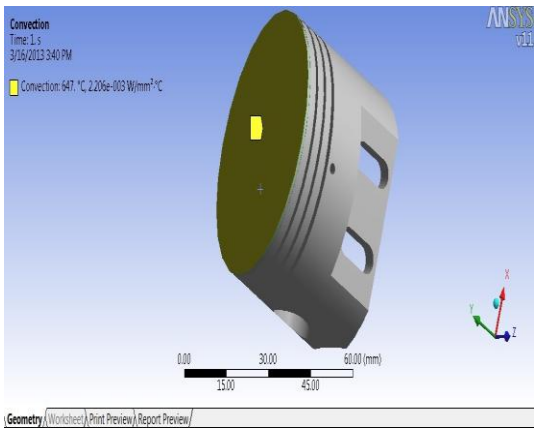

Figure: 3 Boundary Condition at Piston Crown

Temperature distribution

The below fig. 4 shown gives the temperature distribution over the volume of the piston at steady state after and application of thermal loads. The maximum temperature occurs at the top of the piston. A 'MAX' symbol on the temperature distribution chart shows the maximum temperature point. The minimum temperature occurs at the bottom, it is indicated by 'MIN'. An interesting feature in this temperature distribution chart is the combustion chamber. Even though the working medium is at the higher temperatures, the surface temperature at the combustion temperature is comparatively low.

Heat flux

The fig 5 & fig 6 shown above gives the thermal flux distribution over the volume of the piston at steady state after the application of thermal loads. The maximum heat flux occurs at the first ring of the piston. A 'MAX' symbol on the heat flux distribution chart shows the maximum heat flux point. The minimum heat flux occurs at the bottom, it is indicated by 'MIN'. An interesting feature in this heat flux distribution chart is the piston ring. Even though the heat transfer co- efficient on the piston ring is very low, the heat flux seems to be very high and increasessharply.

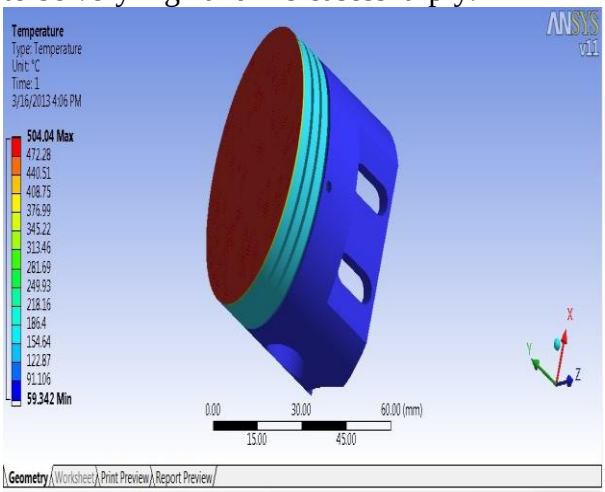

Figure: 4 Temperature Distribution

Near the edge of the first ring (compression ring). Similarly there is a maximum heat flux in the interior region, i.e. in the edges below the combustion chamber.

Total heat flux

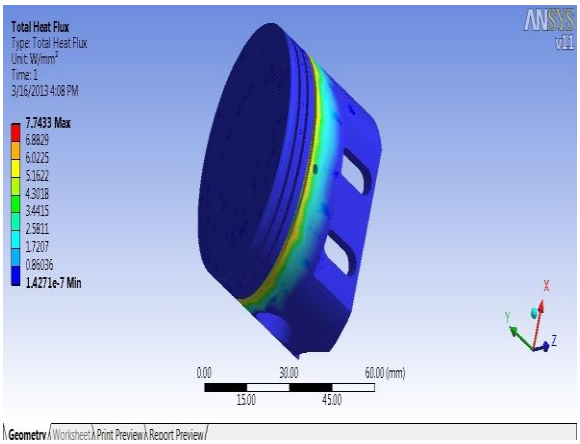

Figure: 5 Total Heat Flux

Directional heat flux

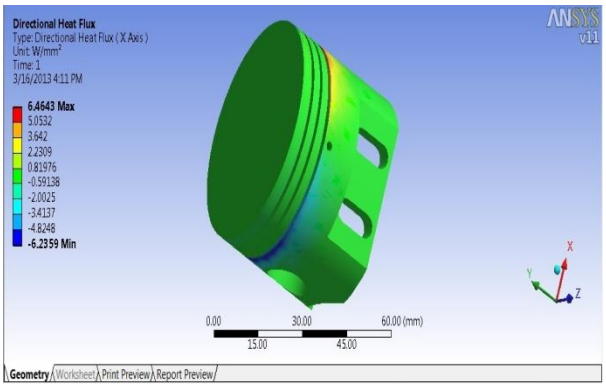

Figure: 6 Directional Heat Flux

Shear stress

A shear stress, denoted τ is defined as the component of stress coplanar with a material cross section. Shear stress arises from the force vector component parallel to the cross section. Normal stress, on the other hand, arises from the force vector component perpendicular or antiparallel to the material cross section on which it acts.

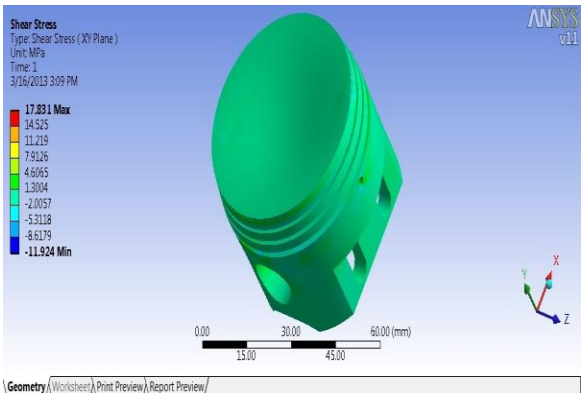

Figure: 7 Shear Stress

Principle stress

They are the stresses normal to a rectangular element of the item being analyzed for stress.

Maximum principle stress and Normal stress

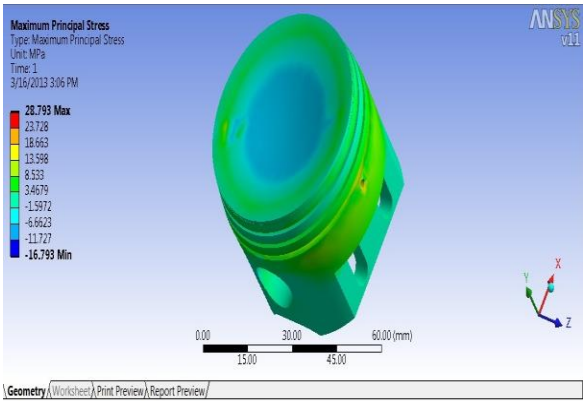

Figure: 8 Maximum Principle Stress

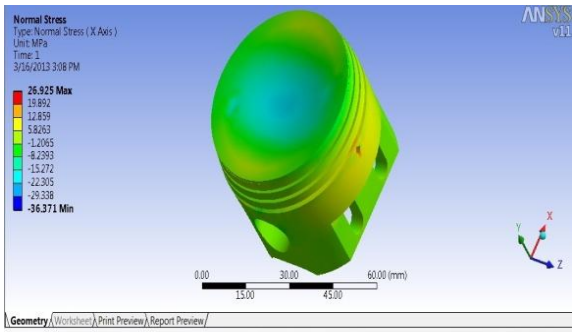

Figure: 9 Normal Stress

Stress intensity

The stress intensity factor, K, is used in fracture mechanics to predict the stress state ("stress intensity") near the tip of a crack caused by a remote load or residual stresses. It is a theoretical construct usually applied to a homogeneous, linear elastic material and is useful for providing a failure criterion for brittle materials, and is a critical technique in the discipline of damage tolerance. The concept can also be applied to materials that exhibit small-scale yielding at a crack tip. The magnitude of K depends on sample geometry, the size and location of the crack, and the magnitude and the modal distribution of loads on the material. Linear elastic theory predicts that the stress distribution (σ_{ij}) near the crack tip, in polar coordinates (r, θ) with origin at the crack tip, has the form

$$\sigma_{ij}(r,\theta) = \frac{K}{\sqrt{2\pi r}} f_{ij}(\theta) + \text{higher order terms}$$

Where K the stress intensity is factor (with units of stress $\times$ length$^{1/2}$) and f_{ij} is a dimensionless quantity that depends on the load and geometry. This relation breaks down very close to the tip (small r) because as r goes to 0, the stress σ_{ij} goes to ∞ . Plastic distortion typically occurs at high stresses and the linear elastic solution is no longer applicable close to the crack tip. However, if the crack-tip plastic zone is small, it can be assumed that the stress distribution near the crack is still given by the above relation.

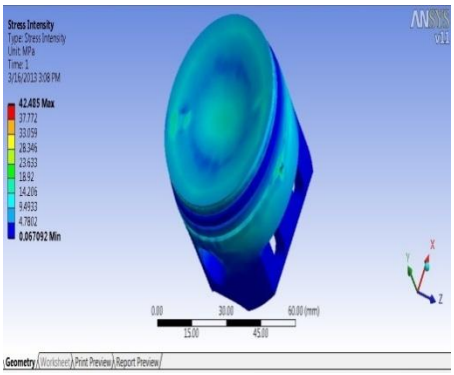

Figure: 10 Stress Intensity

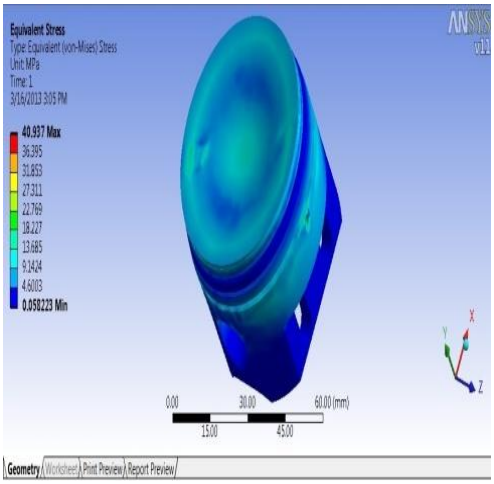

Figure: 11 Equivalent Stress

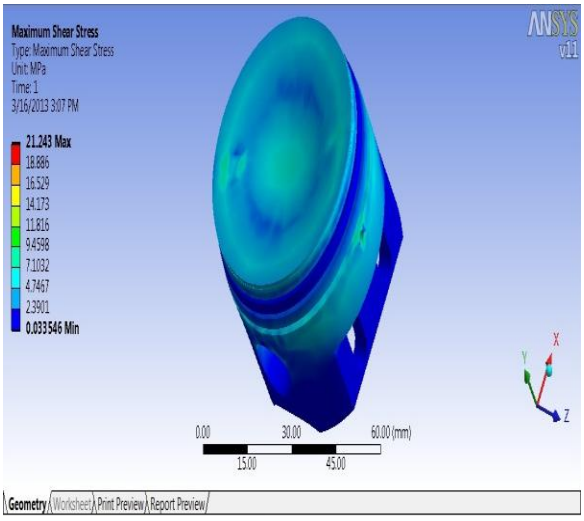

Figure: 12 Maximum Shear Stress

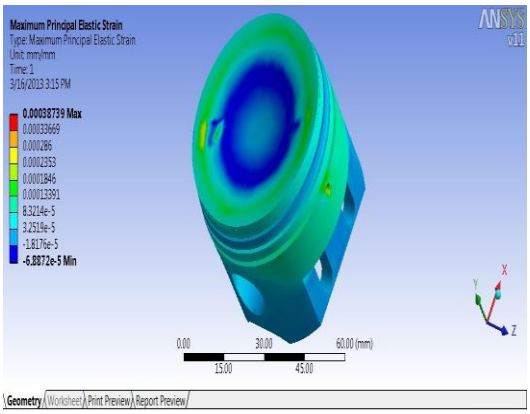

Figure: 13 Maximum Principle Elastic Strain

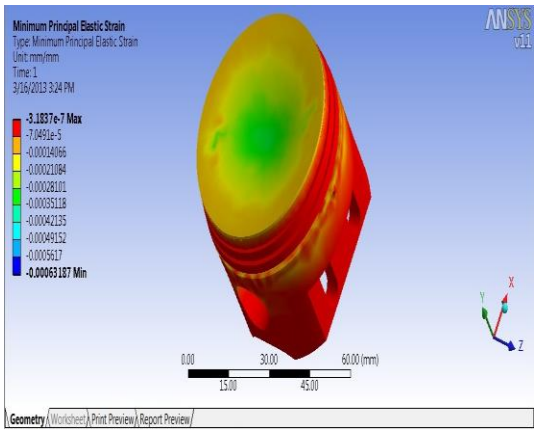

Figure: 14 Minimum Principle Elastic Strain

5. Strain energy

In a molecule, strain energy is released when the constituent atoms are allowed to rearrange themselves in a chemical reaction or a change of chemical conformation in a way that

1. Angle strain,
2. Torsional strain,
3. Ring strain and/or Steric strain,
4. Allylic strain, and
5. Pentane interference

are reduced. The external work done on an elastic member in causing it to distort from its unstressed state is transformed into strain energy which is a form of potential energy.

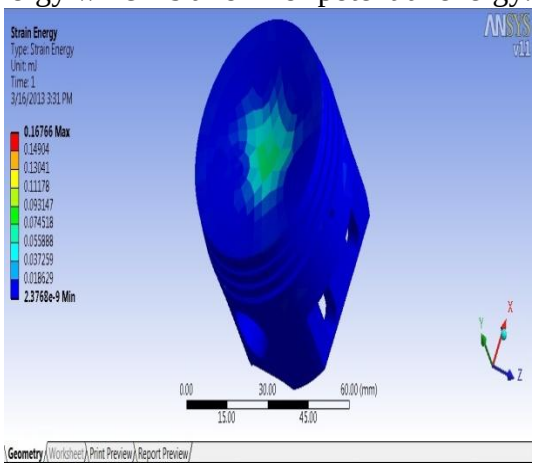

Figure: 15 Strain Energy

The strain energy in the form of elastic deformation is mostly recoverable in the form of mechanical work.

Mass reduction

Mass reduction = Mass of the Existing piston - Mass of the Modified piston

= 113.69 – 109.05

= 4.64 gm

Results and discussions

We havecomparedtheobtained result of thermal & structural analysis of existing piston and modified piston. The thermal analysis, structural analysis, Stress distributions were calculated and tabulated below.

Table 3: Thermal analysis

Properties	**Directional Heat Flux (W/mm^2)**		**Total Heat Flux (^oC)**		**Temperature Distribution (W/mm^2)**	
	MAX	MIN	MAX	MIN	MAX	MIN
Existing Piston	0.0052658	-0.0069654	0.0114	0.00057086	450	159.05
Modified Piston	6.4643	-6.2359	7.7433	$1.4271\times e^{-7}$	504.04	59.342

Table 4: Thermal Analysis

Properties	**Directional Deformation (mm)**		**Equivalent Stress (MPa)**		**Maximum Principle Elastic Strain (mm/mm)**	
	MAX	MIN	MAX	MIN	MAX	MIN
Existing Piston	1.1457	-1.1125×e-9	4.2078×e-5	6.5143×e-8	1.3659×e-10	-6.6743×e-12
Modified Piston	0.0035151	-0.0035635	40.937	0.058223	0.00038739	6.8872×e-5

Table 5: Structural analysis

Properties	**Maximum Principle Stress (MPa)**		**Maximum Shear Stress (MPa)**		**Minimum Principle Elastic Strain (mm/mm)**	
	MAX	MIN	MAX	MIN	MAX	MIN
Existing Piston	$2.7481\times e^{-5}$	$-9.8709\times e^{-6}$	2.1395×e-5	$3.5270\times e^{-8}$	$-1.2e^{-13}$	-2.14
Modified Piston	28.793	-16.793	0.033543	21.243	$-3.1837e^{-7}$	-0.00063187

Table 6: Structural analysis

Properties	**Shear Stress (MPa)**		**Normal Stress (MPa)**		**Strain Energy (mJ)**	
	MAX	MIN	MAX	MIN	MAX	MIN
Existing Piston	$9.516\times e^{-6}$	$-1.338\times e^{-5}$	$2.659\times e^{-5}$	$-3.285\times e^{-5}$	$6.847\times e^{-14}$	$6.3715\times e^{-22}$
Modified	17.831	-11.924	26.925	-36.371	0.16766	$2.3768\times e^{-9}$

Table 7: Structural analysis

Properties	**Stress Intensity (MPa)**		**Total Deformation (m)**		**Mass (gm)**
	MAX	MIN	MAX	MIN	
Existing Piston	$4.2789\times e^{-5}$	$7.0548\times e^{-8}$	5.008	2.377	**113.69**

Modified Piston	42.485	0.067092	0.014278	$2.2011\times e^{-6}$	**109.05**

Conclusion

The existing piston is redesigned using Pro-E software and analyzed by ansys software. The coating of ceramic (magnesium oxide (MgO) and zirconium oxide (ZiO)) over existing aluminum alloy piston is done and behavior is analyzed to improve the performance of the given engine. Thermal analyses results indicate that the coated section of the piston, which is close to the crevice and crown regions, cause an increase in the temperature. It is therefore concluded that this temperature increase leads to an increase in air fuel mixture temperature in these sections and thus unburned charge oxidation near the entrance of the clearance increases. As a result of increase in temperature, a slight amount of decrease in carbon monoxide emission may be expected since CO oxidation reactions strongly depend on temperature.

References

1. Bhaumik Patel, AshwinBhabhorDESIGN and Prediction Of Temperature Distribution Of Piston Of Reciprocating Air Compressor, International journal of Advanced Engineering.IJAERS/Vol. I/ Issue III/April-June, 2012/172-174.
2. P. Gustof, A. HornikThe influence of the engine load on value and temperature distribution in the piston of the turbocharged Diesel engine.
3. EkremBuyukkaya ,MuhammetCerit "Thermal analysis of a ceramic coating diesel engine piston using 3-D finite element method" Surface and coatings technology, june 2007.
4. MuhammetCerit "Thermo mechanical analysis of a partially ceramic coated piston used in an SI engine" ,Surface& coatings Technology, december 2010.
5. M.M.Ragman, A.K.Arifin,N.Jamaludin"Fatique life prediction of two stroke free piston engine mounting using frequency response approach" European journal of scientific research, Vol 22 No.4, 2008.
6. Mirowslawkarczewski,Krzysztofkolinskijercywalentynowcisz "Optical analysis of combustion engine elements" journal of KONES Powertrain and transport , Vol 18, No.1, 2011.
7. Jing Yang, Yi Wang, "Heat load analysis of piston based on the ANSYS", Advanced materials research, Vol 199-200, 2011. EkremBuyukkaya, MuhammetCerit, Theoretical analysis of ceramic coated petrol engine piston using finite element method, SakaryaUniversity, Engineering Faculty, Department of Mechanical Engineering, Esentepe Campus, Sakarya 54187, Turkey (2007).
8. ImdatTaymaz, The effect of thermal barrier coatings on Petrol engine performance, Faculty of Engineering, University of Sakarya, EsentepeKampusu, 54178, Adapazan, Turkey (1993).